CLM-P758

CLM-P758

UKAEA

Preprint

LOW VOLTAGE START-UP IN THE CLEO TOKAMAK USING ECRH

B. LLOYD
T. EDLINGTON

CULHAM LABORATORY
Abingdon, Oxfordshire

1985

CLM-P 758

LOW VOLTAGE START-UP IN THE CLEO TOKAMAK USING ECRH

B Lloyd and T Edlington

Culham Laboratory, Abingdon, Oxon, OX14 3DB, UK

(Euratom/UKAEA Fusion Association)

Abstract

Studies of ECRH-assisted start-up in the CLEO tokamak have resulted in the production of well-controlled discharges with $I_p \sim 13$ kA, $\bar{n}_e \sim 5 \times 10^{18} m^{-3}$ in the presence of a loop voltage $V_\ell < 2V$ throughout. The average loop voltage during the start-up phase is ~ 1.1 V, corresponding to an electric field E $\sim$ 0.19 V/m, and results in an average rate of current rise of $dI_p/dt \sim 0.44$ MA/s. Calculated over the whole of the current rise phase there is a $\sim$ 50% reduction in volt-second consumption when compared with the best case in the absence of rf power. It is estimated that during the plasma current rise $\sim$ 30-50% of the electromagnetic energy input from the poloidal field system is converted to stored magnetic energy.

(Submitted for publication in Plasma Physics and Controlled Fusion)

August 1985

Introduction

There is considerable interest in the development of low voltage start-up scenarios for tokamak devices. Significant reductions in the voltage required for breakdown and in the flux consumption during the current rise phase can lead to substantial savings in the cost of the poloidal field system and permit discharge pulses of greater duration to be obtained. Low voltage start-up is particularly important in reactors in order to avoid problems with the superconducting coils. If the applied voltage necessary for start-up and maintenance of the discharge can be reduced to a sufficiently low value, one can employ a continuous low-resistance vacuum vessel which represents a significant simplification over the usual bellows-type assembly. Apart from the increased mechanical strength of the vessel itself, the impact of a plasma disruption on the remainder of the tokamak assembly is much reduced.

The most successful start-up experiments to date were carried out using injection of lower-hybrid waves on PLT (JOBES et al, 1984) where it was possible to establish a plasma of line-averaged electron density $\bar{n}_e \sim 7 \times 10^{17} m^{-3}$ carrying a current of ~ 100 kA, in the absence of an applied primary voltage, by relying upon direct current drive by the waves (FISCH, 1978). Similar, but more modest, results have been achieved on WT-2 (KUBO et al, 1983) and JIPPT-II (TOI et al, 1984) using a combination of ECRH and lower hybrid current drive. Previous experiments with ECRH preionisation alone (BULYGINSKII et al, 1980; CHO et al, 1980; GILGENBACH et al, 1981; HOLLY et al, 1981; ROBINSON et al, 1982; TANAKA et al, 1982) have resulted in a reduction of typically $\lesssim$ 50% in the initial voltage with generally a smaller reduction in the overall flux consumption during the current rise phase. We report here the establishment of ~ 13 kA discharges at $\bar{n}_e \lesssim 5 \times 10^{18} m^{-3}$ in CLEO tokamak with a loop voltage of less than 2V, which represents a significant improvement over previous results obtained with preionisation. In addition a large reduction in the flux consumption is achieved.

Experimental Details

The CLEO device has been described in detail elsewhere (REYNOLDS et al, 1975). Although originally designed as an ℓ=3 stellarator it now operates primarily as an iron-core tokamak of major radius R_0 = 0.9m and minor radius a = 0.13m as defined by two poloidal limiters placed 180° apart toroidally. Feedback control of plasma current, line-averaged electron density and both vertical and horizontal plasma position allow well-controlled reproducible plasmas to be established. The present series of experiments was carried out with the aid of an EMI-Varian 28 GHz gyrotron capable of providing 200 kW of rf power for pulse lengths of up to 40 ms. The radiation was injected along a major radius from the low field side of the torus through open-ended oversized circular waveguide. The power was transmitted to the antenna in the form of the circularly polarised TE_{01} mode. Hence the resulting antenna pattern is rather broad and both the ordinary (O) and extraordinary (X) modes are excited in the plasma.

The cyclotron resonant field for 28 GHz is 1.0T. However, the work described here was carried out with a magnetic field on axis of $\sim$ 0.9T so that the cyclotron resonance was inwardly displaced $\sim$ 0.09 m from the minor axis (ie at $(R-R_0)/a \sim -0.7$). There is substantial evidence from previous preionisation experiments (ANISIMOV et al, 1973; GILGENBACH et al, 1981; RIVIERE et al, 1977) that although breakdown occurs initially at the electron cyclotron layer ($\omega = \omega_{ce} \equiv eB/m$), as the electron density builds up the region of microwave power deposition moves to the vicinity of the upper hybrid resonance layer (given by $\omega^2 = \omega^2_{UH} \equiv \omega^2_{pe} + \omega^2_{ce}$ where $\omega^2_{pe} \equiv (\frac{n_e e^2}{\varepsilon_0 m})$ is the square of the plasma frequency) which itself becomes further and further detached from the cyclotron layer. As a result it has been found that the optimum conditions for plasma formation coincide with a substantial displacement of the electron cyclotron resonance layer from the centre of the vacuum vessel towards the torus major axis (ATKINSON et al, 1981). During preionisation, when the electron temperature is still very low, the main absorption mechanism is thought to be associated with conversion of the X-mode to an electron Bernstein wave at the upper hybrid resonance (UHR) and subsequent damping of the Bernstein wave between the UHR and the cyclotron layer (STIX, 1965). The Bernstein wave cannot propagate on the high field side of the cyclotron resonance so with the resonant magnetic field located at the minor axis of the torus the microwave heating is effectively restricted to less than half of the plasma volume which may explain the less than optimum absorption efficiency in this case (ATKINSON et al, 1981). Previous results have been found to be relatively insensitive to the polarisation of the launched radiation (CHO et al, 1980; RIVIERE et al, 1977) which is almost certainly related to the fact that when there is low single pass absorption the radiation is rapidly depolarised after reflections from the smooth highly conducting vacuum vessel wall (COSTLEY et al, 1974).

Experimental Results

The beneficial effects of ECRH-assisted start-up are clearly illustrated in Fig 1. An 80 kW, 20 ms pulse of rf power is injected at a time t = 4ms and breaks down an initial prefill of deuterium to a central line-averaged electron density of $\bar{n}_e \sim 0.9 \times 10^{18} m^{-3}$ in a toroidal magnetic field on axis of $B_{\phi o} = 0.895T$. In this preionisation phase a small plasma current of $I_p \lesssim 15A$ is detected. Such currents have been observed previously (KUBO et al, 1983) and may be associated with an asymmetric loss of particles in the presence of toroidal and vertical magnetic fields (TANAKA et al, 1985; WILHELM et al, 1984). In the present experiment there is a small vertical field during the preionisation phase resulting from the bias applied to the iron core before plasma current induction. The plasma current feedback system is triggered at t = 13ms and provides the initial rate of current rise of ~ 750 kA/s. Capacitor banks are discharged into a separate primary winding at 22ms, 51ms and 81ms in order to assist the feedback system. The plasma current reaches its programmed flat-top level of 13.2 kA at 42.8ms (ie, 29.8ms after initiation) representing an average rate of current rise of ~ 440 kA/s during the start-up phase of the discharge. Throughout this phase the loop voltage is typically $V_\ell \sim 1.1V$ as measured by a single-turn loop of radius 0.9m located a distance b = 0.21m vertically above the minor axis. The flux consumption during the plasma current rise is

$$\Delta\Phi = \int V_\ell dt \sim 0.033 \text{ Vs}.$$

Neglecting stray fields, and for a constant plasma position, the voltage at the surface of the plasma, V_s, may be estimated from the relation

$$V_s = V_\ell - L_a dI_p/dt$$

where L_a is the inductance associated with the annular region between the plasma surface and the voltage measuring loop ($a \leqslant r \leqslant b$) and is given by

$$L_a \sim \mu_o R_o \ln(b/a) \sim 0.54\mu H$$

The surface voltage for the discharge of Fig 1 is shown in Fig 2. During the current rise $V_s \lesssim 1V$. Once the current has reached the flat-top value of $I_p \sim$ 13.2 kA the density is raised from $\sim 1.1 \times 10^{18} m^{-3}$ to its final feedback - controlled level of $\sim 4.8 \times 10^{18} m^{-3}$ during which time the surface voltage rises to 1.75V.

The surface voltage $V_s \sim 1$ volt, obtained during the start-up period corresponds to an electric field of ~ 0.18 V/m. The flat-top current of $\sim$ 13.2 kA corresponds to a cylindrical limiter safety factor $q_a \sim 6.4$ and for a central q-value $1 \leqslant q_o \leqslant 2$ the plasma internal inductance is then estimated to be $1.05 \geqslant L_{int} \geqslant 0.72\ \mu H$ for a current density profile of the form $j = j_o\ (1 - r^2/a^2)^{(q_a/q_o)-1}$. Assuming that V_s is constant over the plasma surface, conservation of energy requires

$$\int_0^t V_s I_p dt' = \int_0^t \frac{d}{dt'}(\tfrac{1}{2} L_{int} I_p^2)dt' + \int_0^t (\int_V \underline{j}.\underline{E}d\tau)dt'$$

electromagnetic energy input from poloidal field system	change in stored magnetic energy	resistive losses

$$= (\tfrac{1}{2} L_{int} I_p^2)_{t'=t} + \int_0^t (\int_V \underline{j}.\underline{E}d\tau)dt'$$

Integrating up to the start of the current flat-top for the discharge under consideration gives an efficiency

$$\eta \equiv \tfrac{1}{2} L_{int} I_p^2 / \int V_s I_p dt \sim 0.32 - 0.46$$

for q_0 in the range $2 \geqslant q_0 \geqslant 1$, indicating that approximately 50-70% of the electromagnetic energy input from the poloidal field system appears as resistive losses. Thus there is still scope for further improvements to be made.

Hard X-rays were not detected outside the 2.5 cm thick stainless steel vacuum vessel for the discharge in Fig 1, indicating the absence of runaway electrons with energy $\gtrsim$ 100 keV. However, as seen in Fig 1(g) electron cyclotron emission at 36.3 GHz was detected during the early part of the discharge when the electron density was low. This frequency does not correspond to any cyclotron harmonic for the range of magnetic fields inside the plasma but indicates the presence of 'non-thermal' electrons if it is attributed to Doppler-shifted cyclotron emission.

In Fig 3 the discharge under consideration is compared with the best (ie, lowest voltage at breakdown) yet achieved in the absence of rf power. The final current level and the rate of current rise are approximately the same in the two cases. Without rf power the loop voltage at breakdown is $\sim$ 6.3 V and the flux consumption up to the start of the current flat-top is $\Delta\Phi = \int V_\ell dt \sim$ 0.062 Vs. Estimates of η during the start-up give 0.21 - 0.31 depending, as before, upon the value taken for the central q-value. Thus preionisation results in a 47% reduction in the volt-second consumption and a 48% increase in the fraction of electromagnetic energy input from the poloidal field system which is converted to stored magnetic energy. The voltage required at initiation of the current ramp is reduced by a factor of 5.

With regard to low voltage start-up, the discharges illustrated in Fig 3 are the best obtained so far in CLEO although almost certainly not the optimum. More typically, without preionisation in CLEO the loop voltage at breakdown is $\sim$ 30-40 V and the average rate of current rise during start-up is $\sim$ 0.8 MA/s. The average volt-second consumption in reaching 13.2 kA is $\sim$ 0.111 Vs whilst η is estimated to be typically 0.19 - 0.28 depending upon the value taken for the central q-value. With preionisation the typical corresponding figures are $V_\ell \sim$ 1-4V, $\Delta\Phi \sim$ 0.040Vs and $\eta \sim$ 0.27-0.4.

Summary

The start-up of well-controlled discharges with V_ℓ < 2V has been demonstrated and significant reductions in flux consumption during the current rise phase have been achieved using ECRH. Despite the success of these initial experiments it is estimated that during start-up 50-70% of the electromagnetic energy input from the poloidal field system still goes into resistive losses, which offers the scope for substantial further improvements, perhaps as a result of an extension in the rf pulse length and power injected together with optimisation of the start-up procedure.

Acknowledgements

The authors have benefitted substantially from informative discussions with A C Riviere, D C Robinson and T N Todd and from the assistance and guidance of the CLEO technical team.

References

ANISIMOV A.I., VINOGRADOV N.I. and POLOSKIN B.P. (1973) Soviet Physics Technical Physics 18, 459.

ATKINSON D.W., BRADLEY J.E., DELLIS A.N., JOHNSON P.C., LEES D.J., LLOYD B. et al (1981) Plasma Physics and Controlled Nuclear Fusion Research 1980, Proc 8th Int Conf, Brussels, Vol I, p 153, IAEA, Vienna

BULYGINSKII D.G., LARIONOV M.M., LEVIN L.S., MIKLUKHO O.V., TOKUNOV A.I. and SHUSTOVA N.V. (1980) Soviet Journ Plasma Physics 6, 11.

CHO T., KUBO S., IKEDA M., SAITO T., TERUMICHI Y., HAMADA Y. and TANAKA S. (1980) Physics Letters 77A, 318

COSTLEY A.E., HASTIE R.J., PAUL J.W.M. and CHAMBERLAIN J. (1974) Phys Rev Lett 33, 758

FISCH N.J. (1978) Phys Rev Lett 41, 873

GILGENBACH R.M., READ M.E., HACKETT K.E., LUCEY R.F., GRANATSTEIN V.L., ENGLAND A.C. et al (1981) Nucl Fusion 21, 319

HOLLY D.J., PRAGER S.C., SHEPARD D.A. and SPROTT J.C. (1981) Nucl Fusion 21, 1483

JOBES F. et al (1984) Phys Rev Lett 52, 1005

KUBO S. et al (1983) Phys Rev Lett 50, 1994

REYNOLDS P., MILLWARD P. and HUNT R.R. (1975) Plasma Physics and Controlled Nuclear Fusion Research 1974, Proc 5th Int Conf, Tokyo, Vol II, p 13, IAEA, Vienna.

RIVIERE A.C., ALCOCK M.W. and TODD T.N. (1977) Controlled Fusion and Plasma Physics, Proc 8th Europ Conf, Prague, 1977, Vol I p 119, Czechoslovak Academy of Sciences.

ROBINSON D C , ALCOCK M.W., AINSWORTH N.R., LLOYD B. and MORRIS, A.W. (1982) Proc 3rd Int Symp on Heating in Toroidal Plasmas, Grenoble, 1982, EUR 7979 EN, Vol II, 647

STIX T.H. (1965) Phys Rev Lett 15, 878

TANAKA S. et al (1982) Proc 3rd Int Symp on Heating in Toroidal Plasmas, Grenoble 1982, EUR 7979 EN, Vol II, 733

TANAKA S. et al (1985) Plasma Physics and Controlled Nucléar Fusion Research 1984, Proc 10th Int Conf, London, Vol I, p 623, IAEA, Vienna

TOI K. et al (1984) Phys Rev Lett 52, 2144

WILHELM R., JANZEN G., MULLER G., SCHULLER P.G., SCHWORER K., THUMM M. and ERCKMANN V., (1984) Plasma Physics and Controlled Fusion 26, No 1A, 259

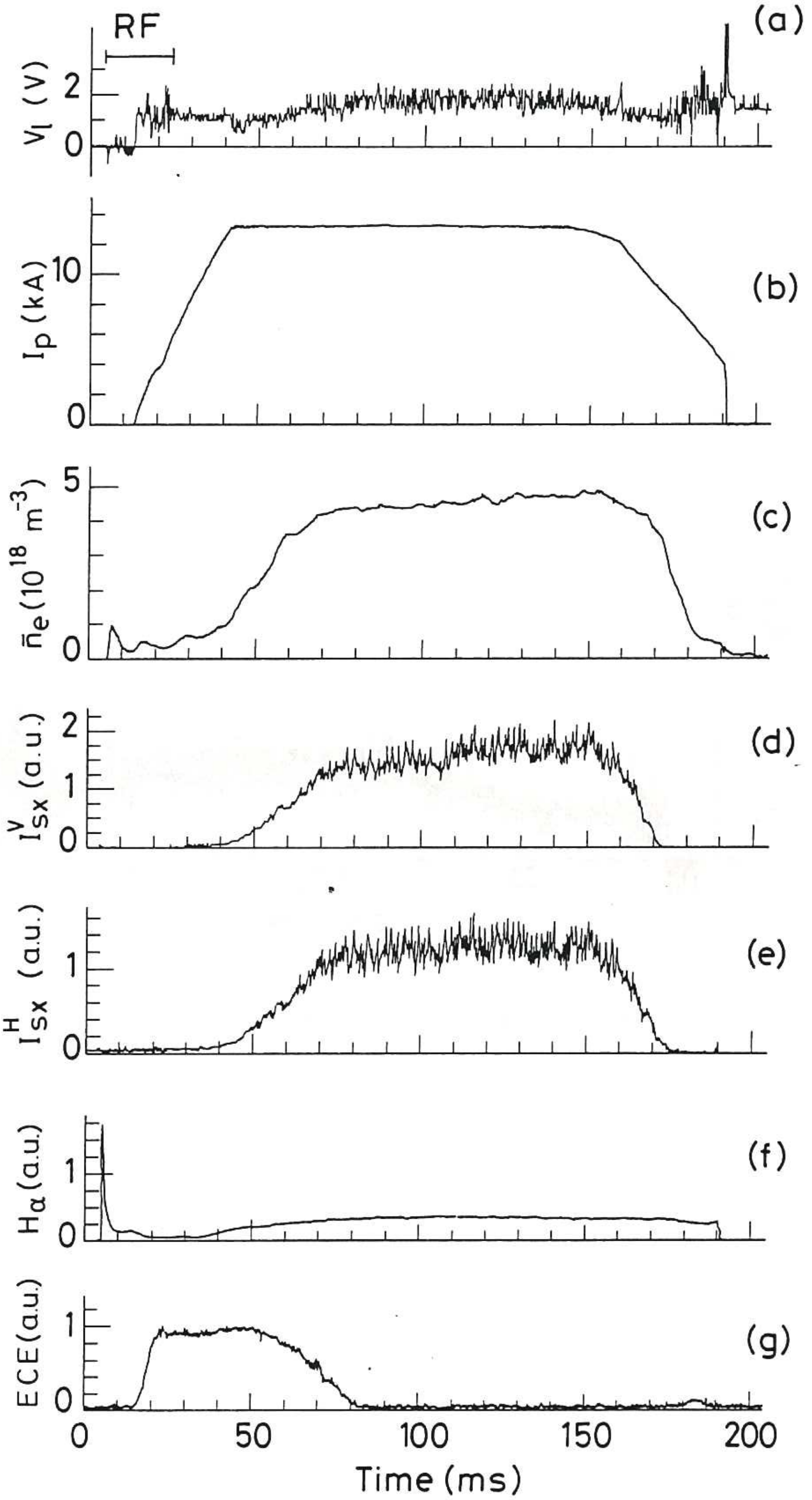

Fig. 1 Low voltage ECRH-assisted start-up: (a) loop voltage, (b) plasma current, (c) line-averaged electron density, (d) vertical soft X-ray emission (r = 0), (e) horizontal soft X-ray emission (r = 0), (f) H_α emission, (g) ECE at 36.3 GHz.

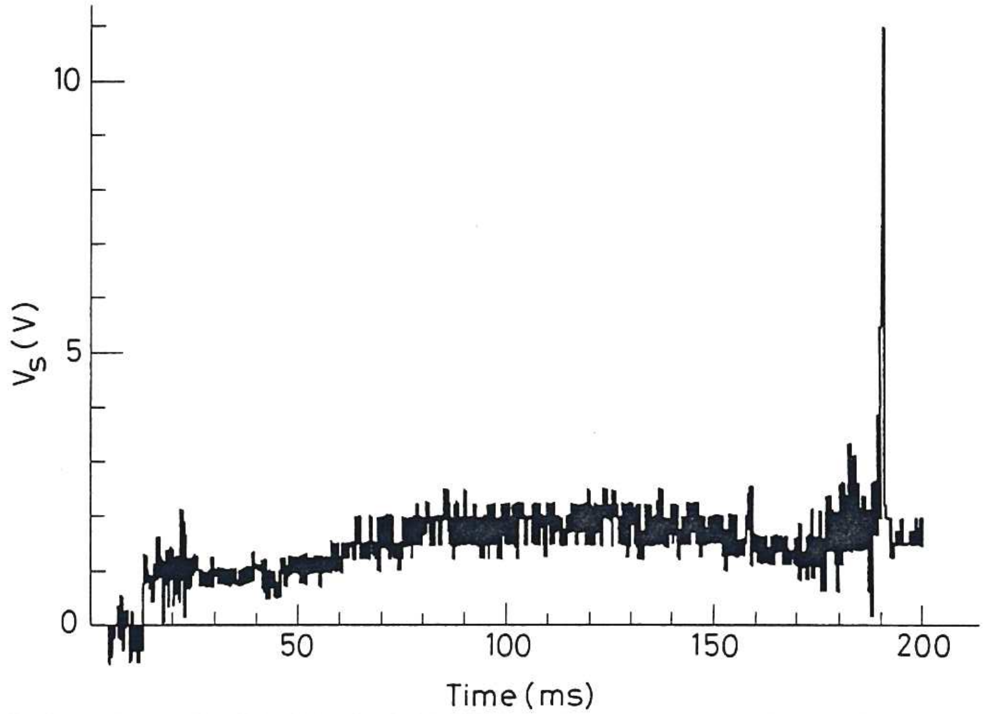

Fig. 2 Surface voltage for the discharge shown in Figure 1.

CLM-P758

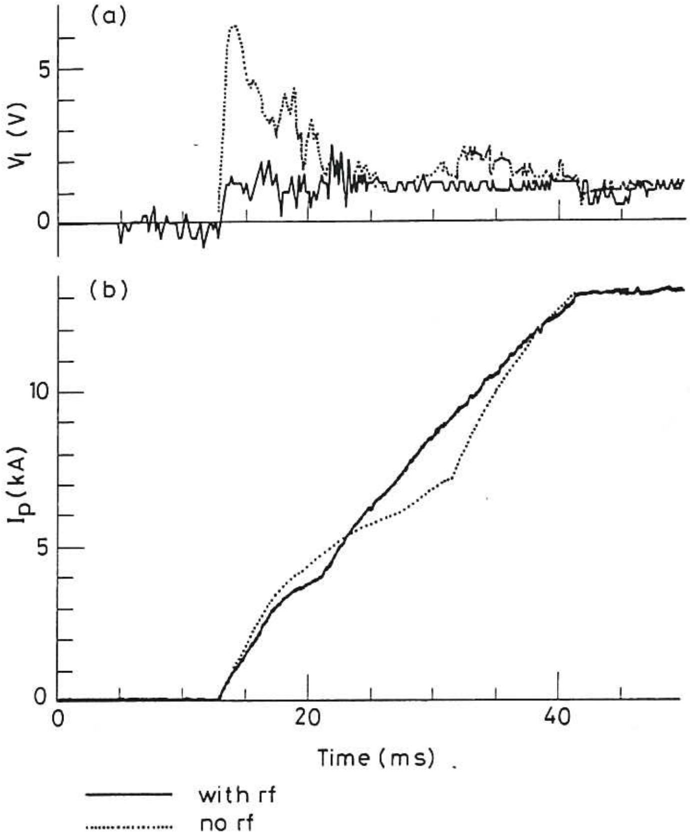

Fig. 3 Comparison of ohmic and ECRH-assisted start-up: (a) loop voltage, (b) plasma current.

CLM-P758

CLM-P757

CLM-P757

UKAEA

Preprint

TURBULENCE DUE TO THE RIPPLING MODE

J. W. CONNOR

CULHAM LABORATORY
Abingdon Oxfordshire
1985

CLM-P757

TURBULENCE DUE TO THE RIPPLING MODE

J W Connor

Culham Laboratory, Abingdon, Oxfordshire, OX14 3DB, UK

(Euratom/UKAEA Fusion Association)

Abstract

Invariance arguments are used to determine the form of the anomalous transport caused by rippling mode turbulence. Remarkably, we find that the thermal diffusivity increases with the parallel thermal conduction. Rippling modes driven by impurity gradients are also considered.

(Submitted for publication in Nuclear Fusion)

August 1985

1. Introduction

Turbulence due to rippling modes [1] has been advanced as an explanation of the fluctuations observed in the edge region of tokamaks [2,3]. Rippling modes are resistive modes driven by a resistivity gradient in the presence of current along the magnetic field. The modes depend on a perturbation of the resistivity in Ohm's law which arises in the presence of a radial gradient of resistivity. If the resistivity depends solely on temperature (ie effects of impurities are ignored [4]) then inclusion of parallel electron thermal conduction $\chi_{\parallel}$ will tend to suppress the resistivity perturbation and hence reduce the growth rate for a given poloidal mode number m [5], where we consider $m >> 1$.

A number of treatments of the non-linear evolution of rippling mode turbulence have appeared in the literature and are summarised in Ref 6, which itself provides the most complete and sophisticated discussion of the so-called resistivity-gradient-driven turbulence.

In particular the authors of Ref 6 quote a formula for thermal diffusivity

$$D \simeq 1.34 \left(\frac{L_s E_0}{L_\eta B_0}\right)^{4/3} \left(\chi_{\parallel} \langle k_{\parallel}'^2\rangle_{rms}\right)^{-1/3} , \qquad (1)$$

where $L_s = \left(\frac{rdq}{Rq^2dr}\right)^{-1}$ and $L_\eta = \left(\frac{d\ell n\eta_0}{dr}\right)^{-1}$ are the magnetic shear and resistivity gradient length scales respectively, E_0 and B_0 are the toroidal electric and magnetic fields and $\langle k_{\parallel}'^2\rangle_{rms}$ is the root mean square average over the turbulent spectrum of $k'_{\parallel} = m/rL_s$. In order to evaluate this formula the authors use the results of a multiple helicity numerical simulation to yield a value for $\langle m^2\rangle_{rms} \simeq 46$. The result is in reasonable accord with experimental measurements.

In this note we wish to apply invariance techniques, previously applied successfully to resistive ballooning and g-mode turbulence [7], to the problem of rippling mode turbulence. This approach provides a valuable perspective for the result (1) demonstrating that it is consistent with the invariance approach, provided its interpretation is appropriately modified. From this new point of view we learn the remarkable result that D increases with $\chi_{\parallel}$!

2. Rippling Mode Turbulence

We consider the electrostatic limit of the reduced resistive mhd equations in cylindrical geometry. Combining Ohm's law with the vorticity equation we find [6]

$$\frac{\rho}{B^2}\frac{d}{dt}\nabla_{\perp}^2\tilde{\phi} = -\frac{1}{\eta_0}\nabla_{\parallel}^{(0)2}\tilde{\phi} - J_z\nabla_{\parallel}^{(0)}\frac{\tilde{\eta}}{\eta_0} , \qquad (2)$$

where $\tilde{\phi}$ is the fluctuating electrostatic potential, the resistivity has been written as a sum of an average part and a rapidly fluctuating part $\eta = \eta_0 + \tilde{\eta}$, ρ is the mass density and J_z and B_z are the current and magnetic field along the axis of the cylinder. The resistivity fluctuation $\tilde{\eta}$ is determined by the electron energy equation

$$\frac{d}{dt}\tilde{\eta} - \chi_{\parallel} \nabla_{\parallel}^{(0)2} \tilde{\eta} = - \frac{1}{rB_z} \frac{\partial \tilde{\phi}}{\partial \theta} \frac{d\eta_0}{dr} \quad . \tag{3}$$

Equations (2) and (3) contain the non-linear convective derivative

$$\frac{d}{dt} = \frac{\partial}{\partial t} + \frac{\nabla_{\perp}\tilde{\phi}}{B_z} \times \underset{\sim}{e}_z \cdot \nabla \equiv \frac{\partial}{\partial t} + \frac{1}{rB_z} \left(\frac{\partial \tilde{\phi}}{\partial \theta}\frac{\partial}{\partial r} - \frac{\partial \tilde{\phi}}{\partial r}\frac{\partial}{\partial \theta}\right) \tag{4}$$

and the parallel and perpendicular gradient operators

$$\nabla_{\parallel}^{(0)} = \frac{B_\theta}{r}\frac{\partial}{\partial \theta} + B_z \frac{\partial}{\partial z} \quad , \qquad \nabla_{\perp}^2 = \frac{\partial^2}{\partial r^2} + \frac{1}{r^2}\frac{\partial^2}{\partial \theta^2} \quad . \tag{5}$$

The fluctuating quantities vary rapidly perpendicular to the magnetic field, but slowly along it.

It is convenient to introduce the dimensionless variables [7]

$$\tau = \frac{B}{Rq\rho^{1/2}} t \quad , \qquad x = (r - r_0)\,\frac{1}{q}\frac{dq}{dr} \quad , \qquad z = R\zeta \quad ,$$

$$\phi = \frac{qR\rho^{1/2}\tilde{\phi}}{r^2 B_z^2} \quad , \qquad \eta = \frac{\tilde{\eta}}{\eta_0} \quad , \tag{6}$$

where r_0 is a reference radius and, in order to simulate a tokamak with major radius R , we have introduced an angle-like variable $\zeta = z/R$ and expressed the shear in terms of the safety factor q. The non-linear equations (2)-(5) take the dimensionless form

$$\frac{d}{d\tau}\nabla_{\perp}^{2}\phi = -S\nabla_{\parallel}^{2}\phi - j\nabla_{\parallel}\eta \quad , \tag{7}$$

$$\frac{d}{d\tau}\eta - K\nabla_{\parallel}^{2}\eta = \frac{1}{\ell}\frac{\partial\phi}{\partial\theta} \quad , \tag{8}$$

where

$$S = \frac{r^{2}B_{\zeta}}{\eta_{0}qR\rho^{1/2}} \quad , \quad j = \frac{RqJ_{\zeta}}{B_{\zeta}} \quad ,$$
$$K = \frac{\chi_{\parallel}\rho^{1/2}}{RqB_{\zeta}} \quad , \quad \frac{1}{\ell} = \frac{r}{\eta_{0}}\frac{d\eta_{0}}{dr} \quad , \tag{9a}$$

$$\frac{d}{d\tau} = \frac{\partial}{\partial\tau} + s\left[\frac{\partial\phi}{\partial\theta}\frac{\partial}{\partial x} - \frac{\partial\phi}{\partial x}\frac{\partial}{\partial\theta}\right] \quad , \tag{9b}$$

$$\nabla_{\perp}^{2} = s^{2}\frac{\partial^{2}}{\partial x^{2}} + \frac{\partial^{2}}{\partial\theta^{2}} \quad , \tag{9c}$$

$$\nabla_{\parallel} = \frac{\partial}{\partial\theta} - q\frac{\partial}{\partial\zeta} - x\frac{\partial}{\partial\theta} \quad , \tag{9d}$$

with $s = \dfrac{r}{q}\dfrac{dq}{dr}$.

We now discuss the invariance properties of these rippling mode equations. Clearly, since the co-ordinate ζ only appears in the expression (9d) for $\nabla_{\parallel}$ we can always scale ζ so that the combination

$(\frac{\partial}{\partial\theta} - q\,\frac{\partial}{\partial\zeta})$ scales as $x\,\frac{\partial}{\partial\theta}$. Equations (7)-(9) are then invariant under four transformations

$$x \rightarrow \alpha_1 x\ ,\ \theta \rightarrow \alpha_1\theta\ ,\ \phi \rightarrow \alpha_1{}^2\phi\ ,\ s \rightarrow \alpha_1{}^{-2}s\ ,\ \ell \rightarrow \alpha_1\ell\ , \qquad A1$$

$$\tau \rightarrow \alpha_2\tau\ ,\ \phi \rightarrow \alpha_2{}^{-1}\phi\ ,\ \eta \rightarrow \alpha_2{}^{-2}\eta\ ,\ s \rightarrow \alpha_2{}^{-1}s\ ,\ K \rightarrow \alpha_2{}^{-1}K\ ,\ \ell \rightarrow \alpha_2{}^2\ell\ , \qquad A2$$

$$\eta \rightarrow \alpha_3\eta\ ,\ j \rightarrow \alpha_3{}^{-1}j\ ,\ \ell \rightarrow \alpha_3{}^{-1}\ell\ , \qquad A3$$

$$\theta \rightarrow \alpha_4\theta\ ,\ \phi \rightarrow \alpha_4{}^2\phi\ ,\ \eta \rightarrow \alpha_4\eta\ ,\ s \rightarrow \alpha_4{}^{-1}s\ ,\ K \rightarrow \alpha_4{}^2K\ . \qquad A4$$

(Note that the scale transformations A1 and A4 do not respect the periodicity of the angle co-ordinates but are permissible because they are applied to short scale fluctuations.)

The turbulent diffusion coefficient transforms as

$$D \sim \frac{(\Delta r)^2}{t} \sim \frac{r^2}{s^2}\,\frac{B}{Rq\rho^{1/2}}\,\frac{(\Delta x)^2}{\tau}\ ,$$

so that D scales as $\alpha_1{}^2\ \alpha_2{}^{-1}\ \alpha_4{}^{-2}$ under the transformations A1 → A4. Thus if we represent D as a function of the local parameters (9a) it must be of the form

$$D = \frac{r^2}{s^2}\,\frac{B}{Rq\rho^{1/2}}\,\frac{1}{S^{5/3}}\,\left(\frac{j}{\ell}\right)^{4/3} F\,\left(\frac{j^2}{K^3 S\ell^2 s^6}\right)\ . \qquad (10)$$

The function F is not yet known but it too can be determined from the invariance principle, if the turbulence is more closely specified. If we employ the customary assumption that the fluctuations vary more rapidly in the (radial) x direction than the (poloidal) θ direction, then equation (9c) reduces to $\nabla_{\perp}^{2} = s^{2}\frac{\partial^{2}}{\partial x^{2}}$ and equations (7)-(9) are invariant under an additional scalar transformation

$$\theta \rightarrow \beta\theta\ ,\ \phi \rightarrow \beta\phi\ ,\ \eta \rightarrow \beta^{2}\eta\ ,\ K \rightarrow \beta^{2}K\ ,\ S \rightarrow \beta^{2}S\ ,\ \ell \rightarrow \beta^{-2}\ell\ . \qquad B1$$

Since D is invariant under the transformation B1 we obtain

$$D = g\frac{r^{2}}{s}\frac{B}{Rq\rho^{1/2}}\frac{1}{S^{3/2}}\left(\frac{j}{\ell}\right)K^{1/2} \qquad (11)$$

or $$D = g\eta^{3/2}\chi_{\parallel}^{1/2}\frac{J}{SB^{2}}Rq\,\rho^{1/2}\frac{d\ell n\eta}{dr} \qquad (12)$$

where g is an undetermined constant.

3. Discussion

The results (1) and (12) are superficially in disagreement: whereas (1) predicts $D \propto \chi_{\parallel}^{-1/3}$, (12) implies $D\ \alpha\ \chi_{\parallel}^{1/2}$. However, this conflict is illusory since the form (1) still contains an unspecified quantity $\langle m^{2}\rangle_{rms}$. We can apply the scaling techniques of section 2 to determine the scaling of $\langle m^{2}\rangle_{rms}$ with the result

$$\langle m^2 \rangle_{rms} \sim \frac{S^{1/2}\, j\, K^{-5/2}}{\ell s^3} \quad . \tag{13}$$

Combining (13) with (1) we recover the result (12), ie $D \propto \chi_{\parallel}^{1/2}$, leading to a dependence

$$D \sim \frac{1}{TB} \quad . \tag{14}$$

Although growth rates at fixed mode number m are reduced by $\chi_{\parallel}$ we find the characteristic value of m reduces with $\chi_{\parallel}$ in such a way as to increase the diffusion. Clearly the condition $m \gg 1$ imposes a limit on the validity of this effect.

Allowing for the substitution (13) we see that the form of the result (1) is determined by invariance arguments and is thus more robust than the particular non-linear calculation might imply. On the other hand the potential advantage of the specific calculation leading to (1) is that it provided a value for the constant g. This depended on a numerical simulation to obtain $\langle m^2 \rangle_{rms}$ which was obtained at a particular set of values of the appropriate parameters S, K, j, ℓ and s. Normalising to this result, it would be possible to extend the validity of this result with the aid of (13).

We have concentrated on comparison with Ref 6 because of the sophistication of the non-linear treatment and therefore the confidence that can be ascribed to the numerical constant calculated therein. However, it is clear that any non-linear treatment of localised turbulence from rippling modes in the presence of $\chi_{\parallel}$, must, with due regard for relation (13), lead to the form (12).

Finally we comment on isothermal impurity gradient driven rippling modes [4,8] which may not be limited to the edge region. In the simplest model $\tilde{\eta}$ is determined by a convection equation for $\dot{Z}_{eff}$ rather than the electron energy equation for T_e. In such a situation $\langle m^2 \rangle_{rms}$ can no longer be controlled by $\chi_{\parallel}$ and one must consider fluctuations for which radial and poloidal variations are comparable in order to determine a scaling for D. Thus the additional assumption needed to obtain the specific result (12) from (10) is no longer required. Application of invariance arguments leads to

$$D \;=\; g'\eta \left(\frac{Rq}{B}\right)^2 \left[\frac{\rho^{1/2}\eta}{s}\, J^2 \left(\frac{d(\ell n Z_{eff})}{dr}\right)^2\right]^{2/3} \qquad (15)$$

where $\frac{d}{dr}\,\ell n\eta \rightarrow \frac{d}{dr}\,\ell n Z_{eff}$ and g' is a constant. Not surprisingly this result corresponds to setting the function $F = g'$, ie independent of $\chi_{\parallel}$, in result (10).

If effects due to the motion of ions and impurities along the field lines are included then friction between the two species plays a similar role to parallel electron thermal conduction in the pure plasma case. One finds [4,8]

$$\chi_{\parallel} \;\rightarrow\; \chi_z \;\equiv\; \frac{{V_{Thi}}^2}{Z^2 \nu_{ii}} \qquad (16)$$

where Z is the impurity charge and V_{Thi} and ν_{ii} are the plasma ion thermal velocity and collision frequency. Application of invariance arguments naturally leads to the results (10) and (12) with the substitution (16), consistent with Ref [8]. Such a result replaces (15) if $\langle m^2\rangle_{rms}$, as estimated from (13) with substitution (16), is large enough for χ_z to be significant, say $\langle m^2\rangle_{rms} > 10^4$ [4].

4. Conclusions

The application of invariance arguments to rippling mode turbulence provides more insight into the meaning and significance of the anomalous transport calculated in Ref 6 and can be used to extend its validity. A surprising result is that the anomalous transport increases with parallel electron thermal conduction: $D \propto \chi_{\parallel}^{1/2}$. Similar techniques have been applied to rippling mode turbulence driven by gradients in Z_{eff}.

Acknowledgement

Useful conversations with Dr P H Diamond on the use of scaling arguments in rippling mode turbulence are acknowledged.

References

[1] FURTH H P, KILLEEN J, ROSENBLUTH M N, Phys Fluids 6 (1963) 459.

[2] ZWEBEN S J, MENYUK C R, TAYLOR R J, Phys Rev Letts 42 (1979) 1270; ZWEBEN S J. TAYLOR R J, Nucl Fusion 21 (1981) 193.

[3] SLUSHER R E, SURKO C M, Phys Rev Letts 40 (1978) 400.

[4] RUTHERFORD P H, in Physics of Plasmas Close to Thermonuclear Conditions, edited by B Coppi (Pergamon Press, Oxford, 1981) Vol 1, p143.

[5] CARRERAS B A, CALLEN J D, GAFFNEY P W, HICKS H R, Phys Fluids 25 (1982) 1231.

[6] GARCIA L, CARRERAS B A, DIAMOND P H, CALLEN J D, Institute for Fusion Studies Report IFSR #146 (1984).

[7] CONNOR J W, TAYLOR J B, Phys Fluids 27 (1984) 2676.

[8] HAHM T S, TERRY P W, DIAMOND P H, Paper 2R-15 Sherwood Theory Conference, Madison (1985).